Color Transparent Monitor using Nanoparticles with Electrically Tunable Viewing Angle

M. Seyyedi
University of Tabriz
Ali Rostami (rostami@tabrizu.ac.ir)
University of Tabriz https://orcid.org/0000-0002-8727-4711
Hamit Mirtagioglu
Bitlis Eren Universitesi

Research Article

Keywords: Transparent Monitor, QDs, Scattering, Electrically Tunable

Posted Date: March 9th, 2022

DOI: https://doi.org/10.21203/rs.3.rs-1353007/v1

Abstract

In this paper, a transparent display with an electrically tunable viewing angle is proposed and numerically simulated. In this work, Si-SiO_2 nanoparticles as core-shell geometry in a periodic array are used. The nanoparticles used in this simulation can be designed in such a way that to absorb less at the blue, green, and red wavelengths. These nanoparticles are stacked horizontally. In this article, by applying a certain amount of voltage at different angles to the transparent screen, the user is given the ability to provide the transparent screen so that, by adjusting the viewing angle of the transparent screen, the content on the transparent screen will be hidden from the view of the people next to the user.

I. Introduction

There are several ways to make transparent displays, but almost none have reached mass production because each technology has its unique problems. For example, a transparent display based on OLED technology is expensive and requires more equipment [1–4]. Removing the background screen is a challenge to create a transparent display based on the LCD method [5–8]. One of the new ways to make a transparent display is using nanoparticles. In [9], coated nanoparticles with silica cores and silver shells were used to create a blue wavelength-sensitive transparent display that could scatter blue wavelength incoming light and show it on the screen. With this method, a display with a wider viewing angle than other methods was made with a larger size and lower manufacturing cost by SiO_2-Ag coated nanoparticles. Dolatyari and her colleagues in [10] were able to increase the transparency of the transparent display by increasing the dispersion cross-section and decreasing the absorption cross-section by using spherical silica-silicon coated nanoparticles in a periodic structure. Eventually, they were able to create a transparent display for blue wavelength with more clarity and a higher figure of merit than the previous works. In [11], Seyyedi et al. were able to significantly increase the scattering cross-section relative to the periodic array by changing the array and position of the nanoparticles and using spherical silica-silicon nanoparticles. Also, by re-examining the size of the nanoparticles, they were able to reach a sharper and narrower peak of scattering cross-section peak at the blue wavelength than in the previous articles. As shown in [12], by changing the morphology of nanoparticles, Prolate Ellipse nanoparticles show higher scattering and lower adsorption cross-section than other nanoparticle morphologies. In [13], Chen et al., by changing the polarization of gold-silver coated elliptical nanoparticles, were able to achieve a greater scattering cross-section and create a red wavelength-sensitive transparent display. In [14], different combinations of nanoparticles were simulated, and a suitable combination was obtained to have high scattering amplitude at three wavelengths of blue, green, and red and lower absorption amplitude for other wavelengths. In [15], more practical arrays such as Gaussian structure were compared with other arrays such as the Fibonacci, the periodic, the Thue-morse, etc. Therefore, using a combination of nanoparticles in the form of a Gaussian array makes it possible to create a transparent display with greater scattering Cross-section at RGB wavelengths. Therefore, many works in the transparent color display have been studied to achieve an optimal structure with the highest scattering and the lowest absorption cross-section with a wide viewing angle. Imagine you are sitting on

the subway and you want to watch a movie or read an article on the transparent screen of your mobile phone or you need to check an essential subject on your transparent display in a public place, but you do not want people sitting next to you to see the contents of your screen. Therefore, in this article, we try to limit the viewing angle of the transparent screen by applying different voltages so that people can communicate with their transparent screen in a personal and individual situation in a public place without being disturbed by anyone else.

Ii. Mathematical Modeling

To calculate far-field angular, scattering, and absorption cross-section, we assume that a plane wave propagates in the z-direction while the wave vector is zero in the x and y directions and k is only in the z-direction (k = 0, 0, k). The amplitude of a complex electric and magnetic field is written based on the incident wave in the form of S and P polarizations according to the coordinates of the (x,y) planes and k = ωn/c [16].

$$E = \begin{bmatrix} E_{\parallel} \\ E_{\perp} \\ 0 \end{bmatrix} e^{ikz}, H = \begin{bmatrix} H_{\parallel} \\ H_{\perp} \\ 0 \end{bmatrix} e^{ikz} = \sqrt{\frac{\epsilon}{\mu}} \begin{bmatrix} -E_{\perp} \\ E_{\parallel} \\ 0 \end{bmatrix} e^{ikz} \quad (1)$$

Where ε, μ, n = $\sqrt{\varepsilon\mu}$represents permittivity, permeability, and refractive index respectively. The incident light hits the x-y planes and is emitted in the z-direction. In this work, we apply an electrical field to x-y planes with different angles to change the viewing angle. For this purpose, we used the E=(V_a/L) V/m equation to estimate the amount of applied voltage. In this relation, V_a and L are externally applied electric potential and length of media in applied voltage direction respectively. The applied field has DC and ac values. The goal is to limit the viewing angle to a specific and slightly limited range. We simulated angle tenability between − 30 to 30 degrees and then generalize for 360 degrees. For this purpose, we considered the screen so that voltage can be applied to the screen separately from both sides, and the screen can be viewed at limited viewing angles. By changing the value of theta, the angle of the applied field can be changed. Note that increasing the applied field does not affect the rate of absorption and scattering cross-section. Therefore, it is easy to change the viewing angle by using voltage or field to the optimal structure obtained from [11–15] without affecting the other acquired optimal factors. For the convenience of making a transparent display, we assumed that the nanoparticles were placed next to each other periodically. As mentioned in previously published articles from this group, the optimal composition of nanoparticles was placed horizontally in a blue-red-green combination. In this regard, according to the results obtained in previous articles, the radius of coated nanoparticles for the core and shell is 50–90 nm, 60–90 nm, and 75–105 nm to have the correct scattering rate for blue, green, and red wavelengths, respectively. We considered the coated nanoparticles to be Si-SiO_2. As we discussed in previous articles and can be seen in Fig. 1, using the structure of the combination of the three

nanoparticles for the periodic structure, we were able to observe the scattering cross-section with sharp peaks in all three wavelengths of blue, red, and green and less absorption cross-section in the rest of the wavelengths. Also, the absorption rate is lower in the whole wavelength range. In the next step, we change the angle of view by applying the field at different angles.

The schematic of this work is shown in Fig. 2. By applying the field at angles of -30 to 30 degrees, the light scattered on the XY plate is reflected around − 30 to 30 degrees, and only in the specified angles can the desired image be seen, and no image can be seen in other angles of view. Depending on the angle of incident light into the structure, we can change the angle of view on the screen and control it. From both sides of the transparent display, the electric field can be applied to the transparent display with different angles and the change of angle can be observed in the scattered light.

Iii. Numerical Simulation

In this paper, we apply electric fields at different angles to the periodic structure of nanoparticles and measure the angle of view for scattered light. We assumed the propagation direction along the Z-axis, the polarization along the X-axis, and the far-field on the XY plane. As shown in Fig. 3–15, by applying an electric field at -30 to 30 degrees from the -X side, the angle of view for scattered field changes to -30 to 30 degrees in the XY plane. The amplitude of the input field is 1 volt per meter. As it is shown in Fig. 3, by applying an electric field at -30 degrees in + X and –X directions, the scattered fields appear in that direction in the X-Y plane. Also, radiation patterns in Y-Z and X-Z planes are considered too.

As it is shown in Fig. 4, by applying an electric field at -25 degrees in + X and –X directions, the scattered fields appear in that direction in the X-Y plane. Also, radiation patterns in Y-Z and X-Z planes are considered too. Considering the radiated patterns distribution, it can be concluded that the considered transparent display has so narrow-band radiation pattern and only the observer in the desired direction can see the image and movie.

As it is shown in Fig. 5, by applying an electric field at -20 degrees in + X and –X directions, the scattered fields appear in that direction in the X-Y plane. Also, radiation patterns in Y-Z and X-Z planes are considered too. The simulated result is similar to the reported case before. The radiated pattern is narrowband and it is very nice for some applications.

Considering Fig. 6, by applying an electric field at -15 degrees in + X and –X directions, the scattered fields appear in that direction in the X-Y plane. Also, radiation patterns in Y-Z and X-Z planes are considered too. In this case, the radiation pattern in the X-Z plane is enhanced versus in previous cases.

Considering Fig. 7, by applying an electric field at -10 degrees in + X and –X directions, the scattered fields appear in that direction in the X-Y plane. Also, radiation patterns in Y-Z and X-Z planes are considered too. In this case, the radiation pattern in the X-Z plane is enhanced versus in previous cases.

Considering Fig. 8, by applying an electric field at -5 degrees in + X and –X directions, the scattered fields appear in that direction in the X-Y plane. Also, radiation patterns in Y-Z and X-Z planes are considered too. In this case, the radiation pattern in the X-Z plane is enhanced versus in previous cases and approximately is the same as the X-Y radiation pattern.

Considering Fig. 9, by applying an electric field at -0 degrees in + X and –X directions, the scattered fields appear in that direction in the X-Y plane. Also, radiation patterns in Y-Z and X-Z planes are considered too. In this case, the radiation pattern in the X-Z plane is exactly the same as the X-Y radiation pattern.

Considering Fig. 10, by applying an electric field at + 5 degrees in + X and –X directions, the scattered fields appear in that direction in the X-Y plane. Also, radiation patterns in Y-Z and X-Z planes are considered too. In this case, the radiation pattern in the X-Z plane is decreased versus in previous cases.

Considering Fig. 11, by applying an electric field at + 10 degrees in + X and –X directions, the scattered fields appear in that direction in the X-Y plane. Also, radiation patterns in Y-Z and X-Z planes are considered too. In this case, the radiation pattern in the X-Z plane is decreased versus in previous cases.

Considering Fig. 12, by applying an electric field at + 15 degrees in + X and –X directions, the scattered fields appear in that direction in the X-Y plane. Also, radiation patterns in Y-Z and X-Z planes are considered too. In this case, the radiation pattern in the X-Z plane is decreased versus in previous cases.

Considering Fig. 13, by applying an electric field at + 20 degrees in + X and –X directions, the scattered fields appear in that direction in the X-Y plane. Also, radiation patterns in Y-Z and X-Z planes are considered too. In this case, the radiation pattern in the X-Z plane is decreased versus in previous cases.

Considering Fig. 14, by applying an electric field at + 25 degrees in + X and –X directions, the scattered fields appear in that direction in the X-Y plane. Also, radiation patterns in Y-Z and X-Z planes are considered too. In this case, the radiation pattern in the X-Z plane is decreased versus in previous cases.

Considering Fig. 15, by applying an electric field at + 30 degrees in + X and –X directions, the scattered fields appear in that direction in the X-Y plane. Also, radiation patterns in Y-Z and X-Z planes are considered too. In this case, the radiation pattern in the X-Z plane is decreased versus in previous cases.

Finally, for different angles in the whole 360 degrees, the following result is obtained for field pattern rotation in the whole 360 degrees.

As shown in Figs. 3–16, by applying an electric field with different angles, the angle of view for scattered light changes. On the other hand, by increasing the number of nanoparticles, the scattering and absorption cross-section can be changed, but the angle of view remains unchanged. Also, changing the amplitude of the electric field does not affect the amount of scattering, absorption, and angle of view.

Conclusion

In this paper, we numerically simulated a transparent display with Si-SiO_2 coated nanoparticles with a limited viewing angle by applying different fields. In this type of display, we used nanoparticles suitable for blue, green, and red wavelengths placed side by side horizontally in a periodic structure. By applying an electric DC field with amplitude value unity per meter and different angles, we were able to adjust the display field of view at a certain angle. We give the ability to users of the transparent screen to use it personally, and other people cannot see the content on the screen.

References

1. J. H. Park, S. D. Baek, J. I. Cho, J. Y. Yoo, S.Y. Yoon, S. Kim, S. Lee, Y.S. Kim, and J.M. Myoung, “Characteristics of transparent encapsulation materials for OLEDs prepared from mesoporous silica nanoparticle-polyurethane acrylate resin composites,” ELSEVIER, Composites Part B 175, 107188, DOI: 10.1016/j.compositesb.2019.107188, 2019.
2. J. MEYER, P. GÖRRN, and T. RIEDL, “Transparent OLED displays,” Woodhead Publishing Limited, DOI: 10.1533/9780857098948.3.512, 2013.
3. D. Yin, Z. Y. Chen, N. R. Jiang, Y. F. Liu, Y.G. Bi, X. L. Zhang, W. Han, J. Feng, and H. B. Sun, “Highly transparent and flexible fabric-based organic light-emitting devices for unnoticeable wearable displays,” ELSEVIER, Organic Electronics 76, 105494, DOI: 10.1016/j.orgel.2019.105494, 2020.
4. H. J. Song, J. Han, G. Lee, J. Sohn, Y. Kwon, M. Choi, and C. Lee, “Enhanced light out-coupling in OLED employing thermal-assisted, self-aggregated silver nanoparticles,” Organic Electronics, S1566-1199(17)30515-3, DOI: 10.1016/j.orgel.2017.10.025, 2017.
5. J. Li, S. Greenberg, and E. Shalin, “A two-sided collaborative transparent display supporting workspace awareness,” International Journal of Human, Computer Studies, Science Direct, Doi: 10.1016/j.ijhcs.2017.01.003, 2017.
6. C. H. Lin, W. B. Lo, K. H. Liu, C.Y. Liu, J. K. Lu, and N, Sugiura, “Novel Transparent LCD with Tunable Transparency,” Wiley online library, SID, V. 43, PP. 1159-1162, DOI: 10.1002/j.2168-0159.2012.tb06001.x, 2012.
7. N. Yamamoto, H. Makino, S. Ozone, A. Ujihara, T. Ito, H. Hokari, T. Maruyama, and T. Yamamoto, “Development of Ga-doped ZnO transparent electrodes for liquid crystal display panels,” ELSEVIER, Thin Solid Films, pp. 4131-4138, DOI: 10.1016/j.tsf.2011.04.067, 2011.
8. J. Heo, J.W. Huh, and T.H. Yoon, “Fast-switching initially-transparent liquid crystal light shutter with crossed patterned electrodes,” AIP Advance 5, 047118, DOI: 10.1063/1.4918277, 2015.
9. C. W. Hsu, B. Zhen, W. Qiu, O. Shapira, B. G. Delacy, J. D. Joannppoulos, and M. Solacic, “transparent displays enabled by resonant nanoparticle scattering,” Nature Communications, DOI. 10.1038/ncomms4152, 2014.
10. M. Dolatyari, A. Jafari, A. Rostami, and A. Klein, “Transparent display using a quasi-array of Si-SiO2 core-shell nanoparticles,” nature, Science reports, DOI. 10.1038/s41598-019-38771-9, 2019.

11. M. Seyyedi, A. Rostami, and S. Matloub, “Comparative study of the transparent display using aperiodic arrays of Si–SiO2 core-shell nanoparticles,” Springer, Optical and Quantum Electronics, https://doi.org/10.1007/s11082-020-02598-w, 2020.
12. M. Seyyedi, A. Rostami, and S. Matloub, “Effect of the morphology of nanoparticles on the performance of the transparent display,” Springer, Optical and Quantum Electronics, https://doi.org/10.1007/s11082-020-02417-2, 2020.
13. M. Chen, H. Yan, P. Zhou, X. Chen, “Transparent Display by the Scattering Effect of Plasmonic Au-Ag Nanoparticles,” springer, Plasmonics, https://doi.org/10.1007/s11468-020-01194-8, 2020.
14. M. Seyyedi, A. Rostami, and S. Matloub, “Effect of different pixel structures on quality of the transparent display implemented by nanoparticles,” Springer, Optical and Quantum Electronics, https://doi.org/10.1007/s11082-021-03152-y, 2021.
15. M. Seyyedi, A. Rostami, and S. Matloub, “Comparative study of the transparent display using Gaussian arrays of Si–SiO2 core-shell nanoparticles and Gaussian radius of nanoparticles,” Springer, Optical and Quantum Electronics, https://doi.org/10.1007/s11082-021-02975-z, 2021.
16. A. Y. Bekshaev, K. Y. Bliokh, and F. Nori, “Mie scattering and optical forces from evanescent fields: A complex-angle approach,” Optics Express, Vol. 21, Issue 6, pp. 7082-7095, Doi:10.1364/OE.21.007082.2013.

Figures

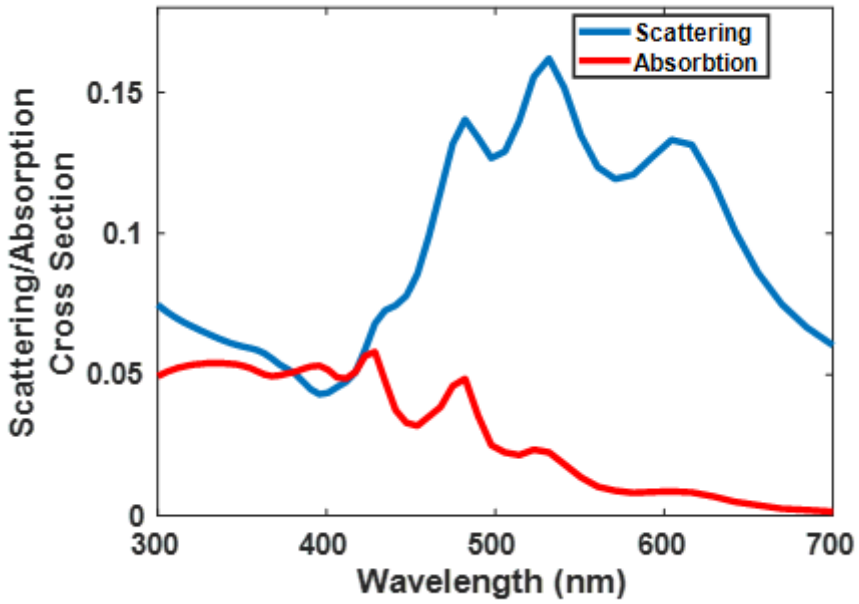

Figure 1

Scattering and absorption cross-section for BRG combination of nanoparticles for the periodic array

Figure 2

The schematic of transparent display with different angles of view

Figure 3

The amount of angle of view for the periodic structure of nanoparticles by applying an electric field at a) -30 degrees from the X side and b) -30 degrees from the -X side

Figure 4

The amount of angle of view for the periodic structure of nanoparticles by applying an electric field at a) -25 degrees from the -X side, and b) -25 degrees from the +X side

Figure 5

The amount of angle of view for the periodic structure of nanoparticles by applying an electric field at a) -20 degrees from the -X side, and b) -20 degrees from the +X side

Figure 6

The amount of angle of view for the periodic structure of nanoparticles by applying an electric field at a) -15 degrees from the -X side, and b) -15 degrees from the +X side

Figure 7

The amount of angle of view for the periodic structure of nanoparticles by applying an electric field at a) -10 degrees from the -X side, and b) -10 degrees from the +X side

Figure 8

The amount of angle of view for the periodic structure of nanoparticles by applying an electric field at a) -5 degrees from the -X side, and b) -5 degrees from the +X side

Figure 9

The amount of angle of view for the periodic structure of nanoparticles by applying an electric field at a) 0 degrees from the -X side, and b) 0 degrees from the +X side

Figure 10

The amount of angle of view for the periodic structure of nanoparticles by applying an electric field at a) 5 degrees from the -X side, and b) 5 degrees from the +X side

Figure 11

The amount of angle of view for the periodic structure of nanoparticles by applying an electric field at a) 10 degrees from the -X side, b) 10 degrees from the +X side

Figure 12

The amount of angle of view for the periodic structure of nanoparticles by applying an electric field at a) 15 degrees from the -X side, and b) 15 degrees from the +X side

Figure 13

The amount of angle of view for the periodic structure of nanoparticles by applying an electric field at a) 20 degrees from the -X side, and b) 20 degrees from the -X side

Figure 14

The amount of angle of view for the periodic structure of nanoparticles by applying an electric field at a) 25 degrees from the -X side, and b) 25 degrees from the -X side

Figure 15

The amount of angle of view for the periodic structure of nanoparticles by applying an electric field at a) 30 degrees from the -X side, and b) 30 degrees from the +X side

Figure 16

The amount of angle of view for the periodic structure of nanoparticles by applying an electric field at different angles in whole 360 degrees with 15-degree distance between them